Progress In Electromagnetics Research M, Vol. 25, 185–195, 2012

SUPER-RESOLUTION IMAGING OF THE GRADED PHOTONIC CRYSTAL WITH NEGATIVE REFRACTION

M. L. Liu[1, 2], M. J. Yun[1, 2, *], F. Xia[1, 2], W. J. Kong[1, 2], Y. Wan[1, 2], J. Liang[1, 2], W. Lv[1, 2], and H. Y. Tan[1, 2]

[1]College of Physics Science, Qingdao University, Qingdao 266071, China

[2]Key Laboratory of Photonics Materials and Technology in Universities of Shandong, Qingdao University, Qingdao 266071, China

Abstract—In this paper, super-resolution imaging and negative refraction by a two-dimensional (2D) triangular lattices graded photonic crystal (GPC) were studied. The graded photonic crystal (GPC) was obtained by varying the radius in each row so that its effective refractive index changes along the transverse direction. By using Plane Wave Expansion (PWE) method and Finite-Difference Time-Domain (FDTD) method, we show that negative refraction and superlensing can be realized in the designed graded photonic crystal. Numerical simulations show that the photonic crystal structures and frequency have an impact on the resolution.

1. INTRODUCTION

Negative refraction of electromagnetic waves and left-handed materials (LHM) were first proposed by Veselago in 1968 [1]. But they did not attract much attention until Pendry put forward that a lossless LHM planar slab with both permittivity and permeability $\varepsilon = \mu = -1$ can be used as a perfect lens [2]. It is well-known that the resolution of conventional imaging systems is inherently restricted by the diffraction limit, where in the spatial information of features smaller than one-half of the wavelength is evanescent and cannot be projected to the far field. A LHM slab appears attractive in providing an effective approach to obtain a superlensing effect that can potentially overcome the diffraction limit inherent in conventional lens and allows for

Received 6 July 2012, Accepted 9 August 2012, Scheduled 13 August 2012

* Corresponding author: Mao Jin Yun (mjyun@qdu.edu.cn).

subwavelength imaging. In the microwave regime, metamaterials can be used to make a superlens capable of the subwavelength imaging [3–6]. But at the optical region, it seems very difficult to make such metallic structures. However, in optical region, it has been shown that two-dimensional photonic crystals (2D PC) can act as effective media with a negative effective refractive index in some frequency regions if being properly designed [7–13]. Luo et al. [8] have studied all-angle negative refraction (AANR) effect in 2D PC that does not employ a negative effective index of refraction. And such an effect is essential for superlens application. To emulate the Veselago's homogeneous negative index medium, Wang et al. proposed a triangular 2D PC consisting of a periodic array of air holes embedded in a dielectric matrix with $\varepsilon = 12.96$ [14]. This PC structure has a fairly isotropic negative effective index of -1 and can get a non-near field image obeying geometric optics. Moreover, some PC slabs with other types of lattice providing a negative effective index of -1 were also reported [15–18]. These PCs are mostly based on circular scatterers. Ref. [12] has demonstrated a PC with a refraction index very close to -1 in a structure of rectangular rods in a triangular lattice, but the refraction index has a small degree of anisotropy. Furthermore, Luo et al. [19] studied the transmission of evanescent waves through a slab of PC with AANR and indicated that the superlensing phenomenon is a result of a subtle synergic interplay between propagating waves and evanescent waves. But for a slab of PC with an effective index of -1, the correlation between the quality of the image and the excitation of PC surface mode is still not clearly understood.

In this work, the graded photonic crystal (GPC) was obtained by varying the radius of dielectric cylinders in each row so that its effective refractive index changes along the transverse direction. The plane wave expansion and the finite difference time domain techniques are applied to do a simulation with the commercial software developed by the Rsoft Design Group. Super-resolution imaging of a point source and negative refraction of a single Gaussian beam incident with different angles are respectively demonstrated by the designed two-dimensional triangular lattices graded photonic crystal. At the same time, the spatial resolution of the graded photonic crystal superlens was analyzed in detail. It is found that frequency of the light has an impact on the resolution.

2. ANALYSIS OF THE DESIGNED GPC

The 2D triangular lattice GPC as shown in Fig. 1(a) is obtained by varying the radius of dielectric cylinders in each row so that its effective

refractive index changes along the transverse direction. Such a stricture is composed of dielectric rods in an air background. The relative permittivity of the rods is taken to be $\varepsilon = 12.25$ and the minimum radius of rod is $r = 0.35a$, where a is the lattice constant. The radii of the dielectric cylinders are identical in each row and modified from the surfaces of PC towards the center as $0.35a$, $0.385a$, $0.42a$ and $0.455a$. Plane Wave Expansion (PWE) method is used to get photonic band structure and equal-frequency contours (EFCs). And the electromagnetic wave propagation is simulated by using the Finite-Difference Time-Domain (FDTD) method.

Figure 1(b) shows the transverse electric (TE) band structure for a triangular two dimensional PC with dielectric rods of radius $r = 0.35a$ (line with square) and $r = 0.455a$ (line with circle) in an air background, the solid line origins from Γ point corresponds to light line. The green line indicates normalized frequency $\omega = 0.295(2\pi c/a)$ corresponding to the effective-negative-index $n_{eff} = -1$, because its equi-frequency contour is nearly circular (in Fig. 2). It can be clearly seen from Fig. 1(b) that the second band extending from 0.21 to $0.36(2\pi c/a)$ has a negative curvature, and the band structure of the PC is shifted to lower frequencies when the radius of the dielectric rods increases from $0.35a$ to $0.455a$. This means that the group velocity $\upsilon_g = \nabla_k \omega(k)$ is negative within this frequency range. So we focus on the second band, the frequency $\omega = 0.295(2\pi c/a)$, where c is the speed of light in vacuum, is the best frequency for the superlensing. And it can be obtained directly by finding the second band interaction with the light line. At this frequency the effective refractive index of the GPC is $n_{eff} = -1$.

It was known that the group velocity of the transmitted electromagnetic waves can be calculated from the equal frequency contours. So the negative refraction can result from special shape EFCs of the hexagonal lattice PC [20]. Taking into account the graded photonic crystal, we choose the radius $= 0.42a$ as supercell. Fig. 2 shows its EFCs computed over the first Brillouin zone for the second band, it can be found that the constant frequency curves, which consist of the allowed propagation modes for a specific frequency, are almost circular and their frequency decrease by increasing the radius. This means that the propagation of the waves is isotropic, and we can define an isotropic effective refractive index using Snell's law. From Figs. 1(b) and 2, it can be observed that the frequency is $\omega = 0.295(2\pi c/a)$ when effective refractive index is $n_{eff} = -1$. It is well known that a LH medium with $n = -1$ perfectly matches to free space (Pendry 2000), and therefore it should not reflects any incoming waves. Hence, the considered GPC structure can leads to an unrestricted superlensing.

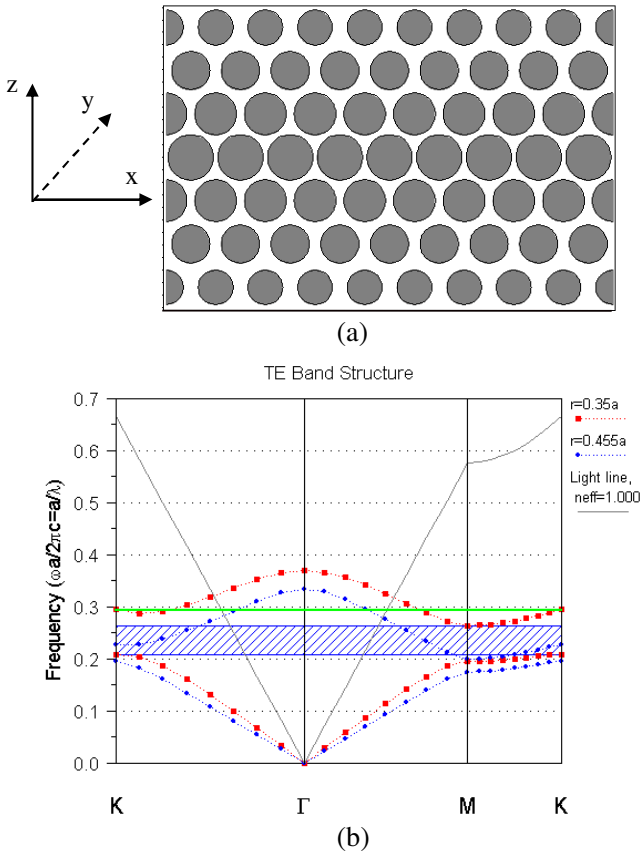

Figure 1. (a) A schematic of the graded photonic crystal with graded dielectric cylinder size, (b) photonic bands of the ordinary PC (not GPC) composed of a triangular lattice of dielectric rods. The red and blue lines are used for the structures with minimum and maximum radius of the rods, respectively. The black line originated from Γ point represents light line. The green line indicates normalized frequency $\omega = 0.295(2\pi c/a)$ corresponding to the effective-negative-index $n_{eff} = -1$.

3. NEGATIVE REFRACTION OF THE DESIGNED GPC

To illustrate the negative refractive and unrestricted superlensing properties, the GPC slab with seven rows of dielectric circular rods in the z-direction and a large enough number of columns to eliminate the boundary effect (40 columns for the case of Gaussian beam incidence simulation in the x-direction) was considered. The simulations are

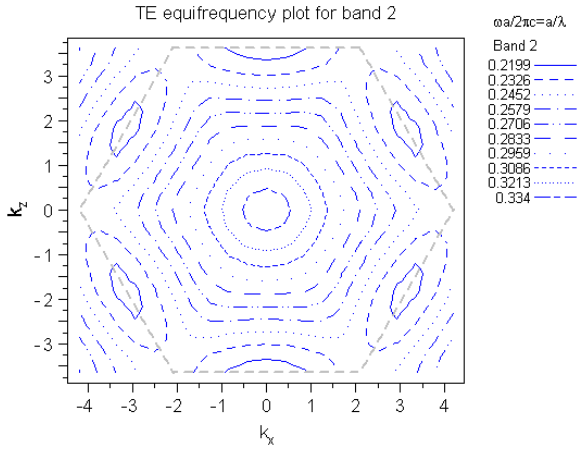

Figure 2. The TE polarized EFCs of the second band of the 2D hexagonal lattice GPC, frequency values are in units of $2\pi c/a$.

carried out by the FDTD method using perfectly matched layer boundary conditions [21, 22]. A Gaussian beam with the frequency $\omega = 0.295(2\pi c/a)$ and width of $10a$ is incident onto the GPC interface with different incident angles. Figs. 3(a), (b) and (c) show the electric field intensities of the Gaussian beam passing through the GPC for different incident angles, 20°, 40° and 60°, respectively. The refracted beam obviously bends to the left side relating to the center of the incident beam, and the outgoing beam keeps a single beam and has a negative shift at the outgoing side even at large incident angle of 60°. However, for very large incident angle there is strong reflection at the GPC interface, which implies this GPC still cannot be seen as a perfectly negative index medium because of poor match to free space. Note that a negative refractive index only represents successfully under certain conditions the refractive properties of the photonic crystal, but one should not expect the validity of such index in Fresnel type of equations, i.e., one does not have a matched PC even with $n = -1$ [23–27].

4. SUPERLENS WITH THE DESIGNED GPC

Negative refraction effect can be utilized in many applications. One such application is superlens. So the superlens can be obtained by using the above designed GPC (Fig. 1(a)) with effective-negative-index of $n_{eff} = -1$. In case of a flat lens with $n = -1$, simple ray-optics predicts the source-image distance to remain constant and equal to twice the lens thickness [6]. Results for periodic PCs showing an almost

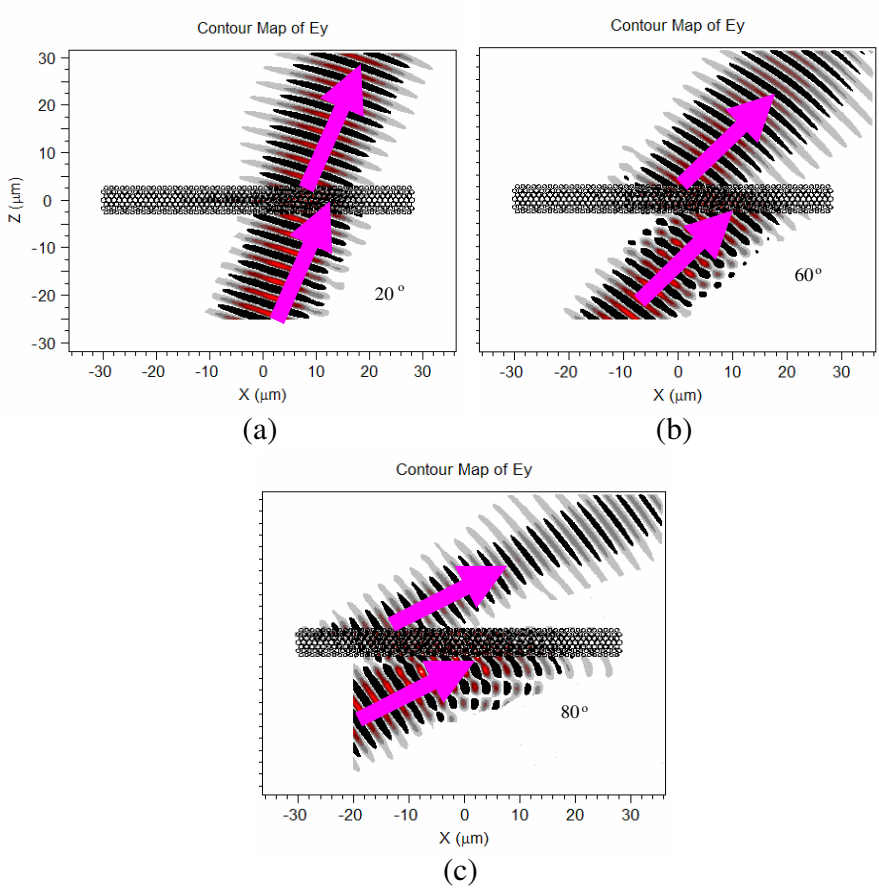

Figure 3. The E fields of a Gaussian beam incoming with different incident angles. (a) $\theta = 20°$, (b) θ=40°, (c) θ= 60°. The structure has 7 rows of dielectric cylinder in the z-direction and 40 columns in the x-direction. The working frequency is $\omega = 0.295 \times 2\pi c/a$ and the Gaussian beam has a width of $10a$.

isotropic refractive response (e.g., see [13]) agree fairly well with this prediction. A continuous-wave point source with $\omega = 0.295(2\pi c/a)$ can be placed at any distances from the left surface of the GPC slab. As we analyzed in Section 3, this frequency is corresponding to the case with effective refractive index of -1. The field distribution of the point source and its image are plotted in Figs. 4(a), (b) and (c) for a point source at distances of $4a$, $6.4a$ and $8.8a$ from the left surface of the GPC slab. It can be found that a visible image spot is formed at $8.8a$, $6.4a$ and $4a$ from the right surface of the GPC slab with the

reverse ordering for the corresponding source positions. So we can conclude that the imaging behaviors depend on the object distance and the GPC slab structure. From Fig. 4 it can be found that the imaging properties are as same as that of the isotropic homogeneous medium with refractive index $n = -1$. Back reflections, represented by additional nodes of intensity and deviations of the wave profiles from circles on the left (source) side of the pictures, are clearly visible in Fig. 4. The field intensity distribution in Fig. 4 is dominated by single cylindrical waves outside the slab, with some standing wave

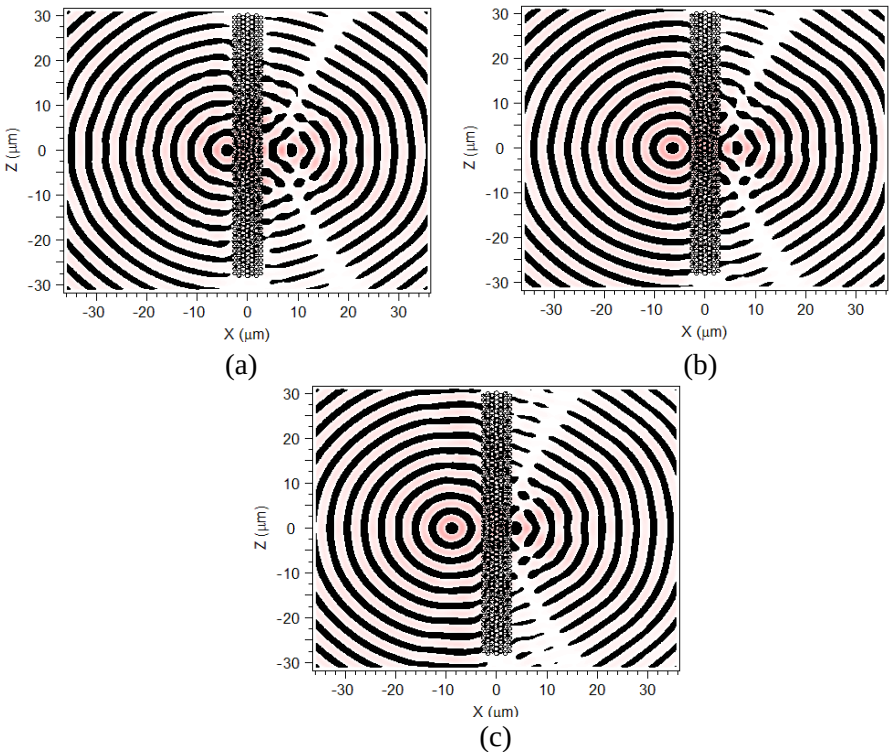

Figure 4. The propagation map (electric field distribution across space) for a slab of the triangular 2D-GPC (the corresponding band structure in Fig. 1(b)), for varying source positions(the left side of the slab). The point source frequency is $\omega = 0.295(2\pi c/a)$. Positions of the images (the right side of the slab) follow the geometric optics analysis, in which the GPC is considered a metamedium with $n = -1$, and Snell's law refraction occurs at each interface. (a) $d = 4a$, (b) $d = 6.4a$, (c) $d = 8.8a$, d is the distance between the source and the center of the slab.

contributions due to back reflections. It was noted by Pendry [2] that superlensing requires the amplification of evanescent waves through the photonic crystal for image formation. While these weak evanescent components do exist in our system, they are difficult to observe in Fig. 4, as they are overwhelmed by the complex pattern of standing and propagating waves inside of the slab. Incident wave cannot be coupled completely to the PC, and the coupling coefficient is highly angular dependent on an interface between air ($n = 1$) and a PC with $n_{eff} = -1$ [28]. This is the reason why the field on the right side of the slab is slightly weaker than the filed on the left side.

In the following, the spatial resolution of the designed GPC slab is analyzed. A continuous-wave point source with the frequency $\omega = 0.295(2\pi c/a)$ is placed at a distance $6.4a$ from the left surface of the GPC slab. Fig. 5 gives the electric field intensity distributions across the image plane for the GPC and ordinary PC, for which we choose $r = 0.42a$ as the radius of dielectric cylinders. The solid line represents the case with the designed GPC slab and dashed line the case with ordinary triangular lattice photonic crystal. It can be found that the full width at half maximum (FWHM) of the image with the designed GPC is about $\Delta = 0.45\lambda$. This value is much better than that of a slab with ordinary triangular lattice photonic crystal in which the FWHM is about $\Delta = 0.67\lambda$. So it can be concluded that the spatial resolution of the designed GPC slab is better than that of the PC slab with ordinary triangular lattice.

In order to test the subwavelength resolution of the designed GPC slab, the imaging property of the point sources with different

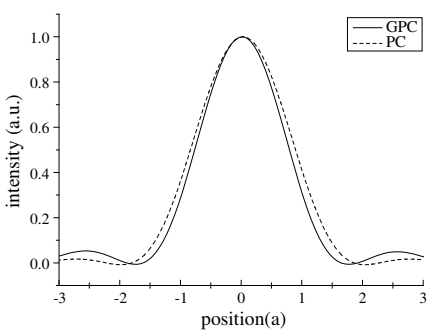

Figure 5. Intensities on the image plane versus the distance from the central maximum. The solid line is for the GPC and the dashed line is for the ordinary PC ($r = 0.42a$).

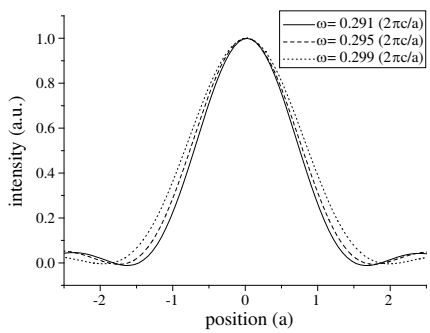

Figure 6. Intensities on the image plane versus the distance from the central maximum for the different frequencies.

frequencies is also studied in this paper. The electric field intensity distributions across the image plane for different frequencies were given in Fig. 6. It can be observed from this figure that the FWHMs of the image with the designed GPC for different frequencies $\omega = 0.291(2\pi c/a)$, $\omega = 0.295(2\pi c/a)$, $\omega = 0.299(2\pi c/a)$ are 0.41λ, 0.45λ and 0.50λ, respectively. So the spatial resolution of the designed GPC slab can be increased by reducing the normalized frequency at which the superlensing occurs This is accordant with Ref. [19].

5. CONCLUSIONS

We designed a graded photonic crystal slab so that it can be used as a perfect lens. Numerical simulations using FDTD methods were also performed to quantitatively analyze the relation between the object and image distances. We also analyzed negative refraction of a single Gaussian beam incidence. Graded photonic crystal has the better resolution compared with the ordinary triangular lattice photonic crystal. It is found that by varying the superlensing frequency, we were able to improve the image resolution. Actually, GPC has potential for optical components and would be efficiently applied to integrated optics devices.

ACKNOWLEDGMENT

This work is supported by the National Natural Science Foundation of China (No. 10904080, No. 11144007), the Distinguished Middle-aged and Young Scientist Encourage and Reward Foundation of Shandong Province, China (No. BS2011DX007) and supported by the State Key Laboratory of Transient Optics and Photonics (No. SKLST201012).

REFERENCES

1. Veselago, V. G., "The electrodynamics of substances with simultaneously negative values of ε and μ," *Sov. Phys. Usp.*, Vol. 10, 509, 1968.
2. Pendry, J. B., "Negative refraction makes perfect lens," *Phys. Rev. Lett.*, Vol. 85, 3966, 2000.
3. Shelby, R. A., D. R. Smith, S. C. Nemat-Nasser, et al., "Microwave transmission through a two-dimensional, isotropic, lefthanded metamaterial," *Appl. Phys. Lett.*, Vol. 78, 489–491, 2001.
4. Houck, A. A., J. B. Brock, and I. L. Chuang, "Experimental

observations of a left-handed material that obeys Snell's law," *Phys. Rev. Lett.*, Vol. 90, 137401, 2003.

5. Aydin, K., I. Bulu, and E. Ozbay, "Subwavelength resolution with a negative-index metamaterial superlens," *Appl. Phys. Lett.*, Vol. 90, 254102, 2007.
6. Lu, W. T. and S. Sridhar, "Flat lens without optical axis: Theory of imaging," *Opt. Express*, Vol. 13, 10673, 2005.
7. Notomi, M., "Theory of light propagation in strongly modulated photonic crystals: Refraction like behavior in the vicinity of the photonic band gap," *Phys. Rev. B*, Vol. 62, 10696, 2000.
8. Luo, C., S. G. Johnson, J. D. Joannopoulos, and J. B. Pendry, "All-angle negative refraction without negative effective index," *Phys. Rev. B*, Vol. 65, 201104, 2002.
9. Foteinopoulou, S. and C. M. Soukoulis, "Negative refraction and left-handed behavior in two-dimensional photonic crystals," *Phys. Rev. B*, Vol. 67, 235107, 2003.
10. Berrier, A., M. Mulot, M. Swillo, M. Qiu, L. Thylen, A. Talneau, and S. Anand, "Negative refraction at infrared wavelengths in a two-dimensional photonic crystal," *Phys. Rev. Lett.*, Vol. 93, 073902, 2004.
11. Hsu, H. T, T. W. Chang, T. J. Yang, B. H. Chu, and C. J. Wu, "Analysis of wave properties in photonic crystal narrowband filters with left-handed defect," *Journal of Electromagnetic Waves and Applications*, Vol. 24, No. 16, 2285–2298, 2010.
12. Dong, G., J. Zhou, X. Yang, and X. Meng, "Multi-refraction with same polarization state in two dimensional triangular photonic crystals," *Progress In Electromagnetics Research*, Vol. 128, 91–103, 2012.
13. Srivastava, R., S. Srivastava, and S. P. Ojha, "Negative refraction by photonic crystal," *Progress In Electromagnetics Research B*, Vol. 2, 15–26, 2008.
14. Wang, X., Z. Ren, and K. Kempa, "Unrestricted superlensing in a triangular two-dimensional photonic crystal," *Opt. Express*, Vol. 12, 2919, 2004.
15. R. Gajic, R. Meisels, F. Kuchar, and K. Hingerl, "All-angle left-handed negative refraction in Kagomé and honeycomb lattice photonic crystals," *Phys. Rev. B*, Vol. 73, 165310, 2006.
16. Jin, Y. and S. L. He, "Negative refraction of complex lattices of dielectric cylinders," *Phy. Lett. A*, Vol. 360, 461, 2007.
17. Dong, G. Y., X. L. Yang, and L. Z. Cai, "Anomalous refractive effects in honeycomb lattice photonic crystals formed

by holographic lithography," *Opt. Express*, Vol. 18, 16302, 2010.

18. Sun, J., Y. F. Shen, J. Chen, L. G. Wang, L. L. Sun, J. Wang, K. Han, and G. Tang, "Imaging properties of a two-dimensional photonic crystal with rectangular air holes embedded in a silicon slab," *Photon. Nanostructures*, Vol. 8, 163, 2010.
19. Luo, C., S. G. Johnson, J. D. Joannopoulos, and J. B. Pendry, "Subwavelength imaging in photonic crystals," *Phys. Rev. B*, Vol. 68, 045115, 2003.
20. Zhang, X., "Image resolution depending on slab thickness and object distance in a two-dimensional photonic-crystal-based superlens," *Phys. Rev. B*, Vol. 70, 195110, 2004.
21. Taflove, A., *Computational Electrodynamics: The Finite-Difference Time-Domain Method*, Artech House, Boston, 1995.
22. Bérenger, J. P., "A perfectly matched layer for the absorption of electromagnetic waves," *J. Comput. Phys.*, Vol. 114, 185, 1994.
23. Cabuz, A. I., E. Centeno, and D. Cassagne, "Superprism effect in bidimensional rectangular photonic crystals," *Appl. Phys. Lett.*, Vol. 84, 2031, 2004.
24. Joannopoulos, J. D., R. D. Meade, and J. N. Winn, *Photonic Crystals: Molding the Flow of Light*, Princeton University Press, Princeton, New Jersey, 1995.
25. Benedicto, J., R. Pollès, A. Moreau, and E. Centeno, "Large negative lateral shifts due to negative refraction," *Opt. Lett.*, Vol. 36, 2539, 2011.
26. Shi, P., K. Huang, and Y. P. Li, "Enhance the resolution of photonic crystal negative refraction imaging by metal grating," *Opt. Lett.*, Vol. 37, 359, 2012.
27. Krayzel, F., R. Pollès, A. Moreau, M. Mihailovic, and G. Granet, "Simulation and analysis of exotic non-specular phenomena," *J. Europ. Opt. Soc. Rap. Public.*, Vol. 5, 10025, 2010.
28. Ruan, Z. C., "Dispersion engineering: Negative refraction and designed surface plasmons in periodic structures," Ph.D. Thesis in Microelectronics and Applied Physics Stockholm, 31–35, Sweden, 2007.